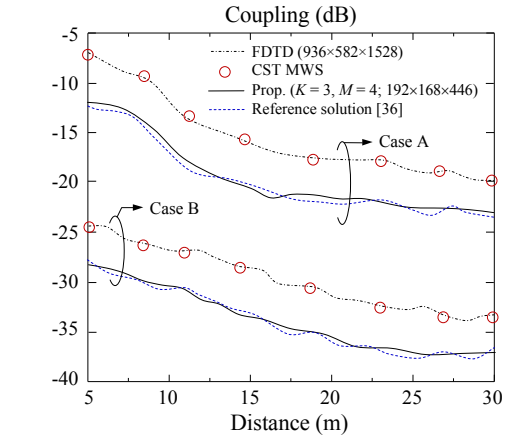


(a)

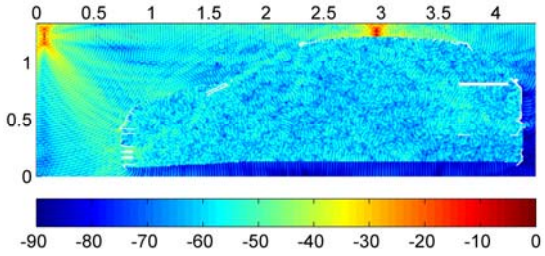

(b)

Figure 27: (a) Coupling between two vehicles versus their distance for two communication link cases (A: antennas mounted on the roofs and B: antennas mounted at the back of the vehicles). (b) Electric field distribution (in dB) at the outer surface of the vehicle for a roof-mounted antenna.

lays in the exchange of information between moving vehicles or between vehicles and infrastructure in order to achieve high levels of efficiency and electromagnetic coupling (Fig. 26b). The antennas of the vehicles are vertically-polarized monopoles that transmit according to the IEEE 802.11p standard, i.e. with a power of 1.0 W EIRP (equivalent isotropic radiated power). For this very large-scale ($56\lambda \times 30\lambda \times 100\lambda$) problem, the overall mesh of our method comprises 192×168×446 ≈ 14.4 million cells (nearly 0.72 GB), while that of the FDTD technique requires 936×582×1528 ≈ 832.4 million cells and around 30 GB. Notice that regarding (12), $a_1 = 0.221067$, $a_2 = 0.038512$, and $a_3 = 0.240421$. Figure 27a presents the electromagnetic coupling between two vehicles versus their distance and compares the results with the reference solution acquired through the formulation of [36] and Fig. 27b shows the electric field distribution at the surface of the vehicle when the antenna is mounted on its roof. Again, the proposed approach offers a significantly more reliable performance than the FDTD one (verified by the CST MWS), despite its finer (almost 93%) discretization.

The final application is concerned with the wave propagation study of an indoor environment, where a wireless local area network (WLAN) operation has been installed. Our site is a typical 9.1×8.5×2.8 m office area with three independent rooms, as depicted in Fig. 28, whose walls are 20 cm thick and have a $\sigma = 30$ mS/m conductivity. Several potential positions (blue numbers in Fig. 29) of the transmitter – modeled as an omnidirectional radiating source – are considered, while

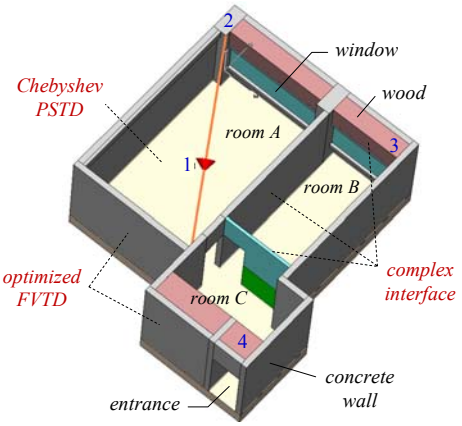


Figure 28: Perspective view of the investigated office area. Modeling regions: complex-interface schemes for the inner walls, the windows, and the wooden structures, optimized FVTD technique for the external walls, and PSTD algorithm for the interior of the domain.

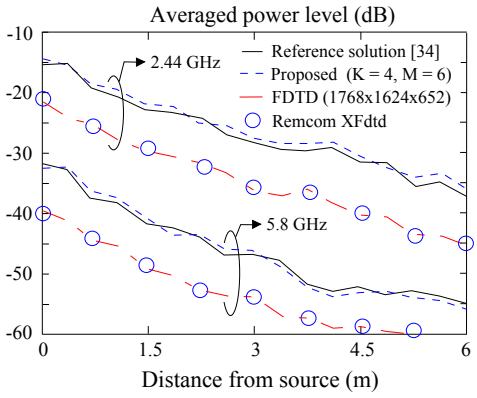


(a)

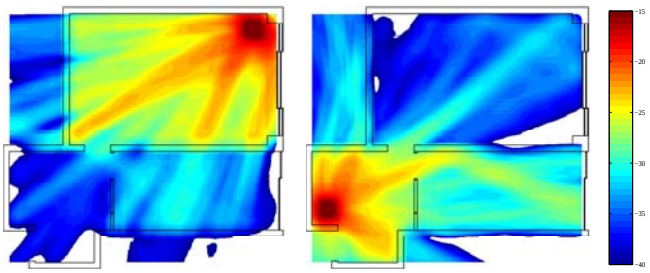

(b) (c)

Figure 29: (a) Received power levels along the path of Fig. 28 and power-coverage maps at (b) 2.44 GHz and (c) 5.8 GHz.

both the 2.44 GHz and the 5.8 GHz case are explored. To implement the proposed method, we select $a_1 = 0.031365$, $a_2 = 0.950086$, $a_3 = -0.418721$, and construct a grid with 388×342×192 ≈ 25.5 million cells (about 1.27 GB). The corresponding FDTD discretization for a resolution of $\lambda/25$ requires a mesh of 1768×1624×652 ≈ 1.87 billion cells and around 67.32 GB. Figure 29a illustrates the received (averaged) power levels along a diagonal path sketched in Fig. 28. Evidently, the hybrid schemes attain a very satisfactory accuracy, compared to the reference solution via the geometrical theory of diffraction [34] and the outcomes of the FDTD approach (validated by the Remcom XFdtd). Moreover, Fig. 29b and 29c show the

power-coverage maps at 2.44 GHz and 5.8 GHz at source locations 2 and 4, respectively, and a dynamic range level from – 40 to –15 dB. Observe the different penetration power levels through the walls of the site for the two frequencies and the smoothness of the plots achieved by our algorithm.

Generally, interpreting the results from the applications studied in this section, it is derived that the conformal hybrid methodology can successfully cope with complex electrically-large structures and realistic arrangements. It is emphasized that all problems can be safely deemed large-scale, since the corresponding FDTD meshes for their adequate discretization range from 55 million to 1.9 billion cells. As already deduced, the proposed technique leads to remarkably coarser (almost 90-93%) lattices and minimizes the undesired dispersion errors up to 10 orders of magnitude, without any exponential instabilities even for simulations lasting for several million time-steps. Consequently, high levels of accuracy are accomplished in contrast to the typical time-domain realizations, which require excessive numbers of cells without being able to provide reliable outcomes. Such assets are proven more significant as the application size becomes larger due to the noteworthy computational savings, thus enabling the analysis of demanding problems by usual limited-memory systems.

## 7. Conclusions

A hybrid time-domain methodology, based on advanced FVTD and PSTD schemes, has been proposed in this paper for the precise design and modeling of large-scale 3-D EMC structures. Established through a low-complexity generalized rationale, the parametric technique introduces new operators with optimal nodal density and media-sensitive interface conditions. In essence, the FVTD approach uses a leap-frog integration scheme – conditionally stable and non-dissipative – that conserves the total charge in a global and local sense. Thus, canonical staggered-meshed formalisms (as in the FDTD algorithm) are efficiently circumvented with the computational overhead limited in reasonable levels. On the other hand, the PSTD concept uses Chebyshev polynomials, through a fast Fourier transform (FFT), instead of the customary finite-difference approximators, to evaluate spatial derivatives in areas of abrupt field variation. Due to its enhanced spectral accuracy, the PSTD technique entails only two cells per wavelength according to the Nyquist sampling theorem and, therefore, can deal with more challenging scenarios. Hence, and as realistic numerical evidence determines, artificial reflection errors are greatly suppressed and very rigorous as well as inexpensive solutions are acquired.

## Acknowledgements

This research has been supported by the Aristotle University of Thessaloniki under grant 87908.

## References

[1] C. Holloway, P. McKenna, R. Dalke, R. Perala, C. Devor, Time-domain modeling, characterization, and measurements of anechoic and semi-anechoic electromagnetic test chambers, *IEEE Trans. Electromagn. Compat.* 44: 102−118, 2002.

[2] C. Buccella, M. Feliziani, F. Maradei, G. Manzi, Magnetic field computation in a physically large domain with thin metallic shields, *IEEE Trans. Magn.* 41: 1708−1711, 2005.

[3] C. Bruns, R. Vahldieck, A closer look at reverberation chambers – simulation and experimental verification," *IEEE Trans. Electromagn. Compat.* 47: 612−626, 2005.

[4] S. Lee, M. Vouvakis, J.-F. Lee, "A non-overlapping domain decomposition method with non matching grids for modeling large arrays, *J. Comp. Phys.* 203: 1–21, 2005.

[5] N. Kantartzis, T. Tsiboukis, E. Kriezis, A topologically consistent class of 3-D higher-order curvilinear FDTD schemes for dispersion-optimized EMC material modelling, *J. Materials Proces. Technol.* 161: 210–217, 2005.

[6] M. Sarto, A. Tamburrano, Innovative test method for the shielding effectiveness measurement of thin films in wide frequency range, *IEEE Trans. Electromagn. Compat.* 48: 331−341, 2006.

[7] B. Lakshminarayanan, D. Mercier, G. Rebeiz, High-reliability miniature RF-MEMS switched capacitors, *IEEE Trans. Microw. Theory Tech.* 56: 971–981, 2008.

[8] S. Lucyszyn, *Advanced RF MEMS*, Cambridge University Press, London, 2010.

[9] A. Duffy, A. Orlandi, H. Sasse, "Offset difference measure enhancement for the feature-selective validation method, *IEEE Trans. Electromagn. Compat.* 50: 413 −415, 2008.

[10] Y. Li, J. Zhu, Q. Yang, Z. Wei, Y. Guo, Y. Wang, Measurement of soft magnetic composite material using an improved 3-D tester with novel sensing coils, *IEEE Trans. Magn.* 46: 1971–1974, 2010.

[11] D. Baumann, C. Fumeuax, R. Vahldieck, Field-based scattering matrix extraction scheme for the FVTD method exploiting a flux-splitting algorithm, *IEEE Trans. Microw. Theory Tech.* 53: 3595–3605, 2005.

[12] D. Firsov, J. LoVetri, O. Jeffrey, V. Okhmatovski, C. Gilmore, W. Chamma, High-order FVTD on unstructured grids using an object-oriented computational engine, *ACES J.* 22: 71−82, 2007.

[13] C. Bommaraju, W. Ackermann, and T. Weiland, Convergence of error in FVTD methods on tetrahedral meshed in 3D, *Proc. Applied Electromagn. Conf. (AEMC)*, pp. 1–4, 2009.

[14] G. Bozza, D. Caviglia, L. Ghelardoni, and M. Pastorino, Cell-centered finite-volume time-domain method, *IEEE Microw. Wireless Compon. Lett.* 20: 477–479, 2010.

[15] I. Jeffrey, J. LoVetri, Interfacting thin-wire and circuit subcell models in unstructured time-domain field solvers, *IEEE Trans. Antennas Propag.* 60: 1−9, 2012.

[16] Q. Liu, G. Zhao, Review of PSTD methods for transient electromagnetics, *Int. J. Numer. Model.* 22: 299−323, 2004.

[17] X. Gao, M. Mirotznik, D. Prather, A method for introducing soft sources in the PSTD algorithm, *IEEE Trans. Antennas Propag.* 52: 1665−1671, 2004.

[18] Y. Fan, B. Ooi, M. Leong, Fast multipole accelerated Chebyshev pseudospectral time domain algorithm, *IET Microw., Antennas Propag*. 1: 763−769, 2007.

[19] D. Vande Ginste, E. Michielssen, F. Olyslager, D. De Zutter, An efficient PML based on multilevel fast multipole algorithm for large microwave structures, *IEEE Trans. Antennas Propag.* 54: 1538−1548, 2006.

[20] Y. Song, N. Nikolova, M. Bakr, Efficient time-domain sensitivity analysis using coarse grids, *ACES J.* 23: 5−15, 2008.

[21] T. Ohtani, K. Taguchi, T. Kashiwa, Y. Kanai, J. Cole, Scattering analysis of large-scale coated cavity using the nonstandard FDTD method, *IEEE Trans. Magn.* 45: 1296 –1299, 2009.

[22] I. Ahmed, E.-H. Khoo, Erping Li, Development of the CPML for the 3-D stable LOD-FDTD method, *IEEE Trans. Antennas Propag.* 58: 832−837, 2010.

[23] R.Hedge, Z. Szabo, Y. Hor, Y. Kiasat, Erping Li, W. Hoefer, The dynamics of nanoscale super-resolution imaging with the superlens, *IEEE Trans. Microw. Theory, Tech.* 59: 2612−2623, 2011.

[24] B. Zhu, J. Lu, Erping Li, Electromagnetic compatibility benchmark-modeling for a dual-die CPU, *IEEE Trans. Electromagn. Compat.* 53: 91−98, 2011.

[25] H. Attia, L. Yousefi, O. Ramahi, "Analytical model for calculating the radiation field of microstrip antennas with artificial magnetic superstrates: Theory and experiment," *IEEE Trans. Antennas Propag.* 59: 1438–1445, 2011.

[26] P. Ding, C. Qiu, S. Zouhdi, Rigorous derivation and fast solution of spatial-domain Green's functions for uniaxial anisotropic multilayers using modified fast Hankel transform method, *IEEE Trans. Microw. Theory, Tech.* 60: 205−217, 2012.

[27] R. Nilavalan, I. Craddock, C. Railton, Quantifying numerical dispersion in non-orthogonal FDTD meshes, *IEE Proc. Microw. Antennas Propag.* 149: 23−27, 2002.

[28] A. Taflove, S. Hagness, *Computational Electrodynamics: The Finite-Difference Time-Domain Method*, Artech House, Norwood, MA, 2005.

[29] W. Yu, R. Mittra, S. Dey, Application of the nonuniform FDTD technique to analysis of coaxial discontinuity structures, *IEEE Trans. Microw. Theory Tech.* 49:207–209, 2001.

[30] N. Kantartzis, T. Tsiboukis, E. Kriezis, An explicit weighted essentially non-oscillatory time-domain algorithm for the 3-D EMC applications with arbitrary media, *IEEE Trans. Magn.* 42, 803−806, 2006.

[31] S. Noelle, W. Rosenbaum, M. Rumpf, 3D adaptive central schemes: Part I. Algorithms for assembling the dual mesh, *Appl. Numer. Math.* 56: 778–799, 2006.

[32] T. Sengupta, S. Bhaumik, U. Shameem, A new compact difference scheme for second derivative in non-uniform grid expressed in self-adjoint form, *J. Comput. Phys.* 230: 1822−1848, 2011.

[33] J.-P. Berenger, An optimized CFS-PML for wave-structure interaction problems, *IEEE Trans. Electromagn. Compat.* 54: 1−8, 2012.

[34] J. van Bladel, *Electromagnetic Fields*, IEEE Press, New York, NJ, 2007.

[35] D. Pozar, *Microwave Engineering*, Wiley, New York, NJ, 2011.

[36] P. Belanovic, D. Valerio, A. Paier, T. Zemen, F. Ricciato, C. Mecklenbrauker, On wireless links for vehicle-to-infrastructure communications, *IEEE Trans. Vehicular Tech.* 59: 269–282, 2010.